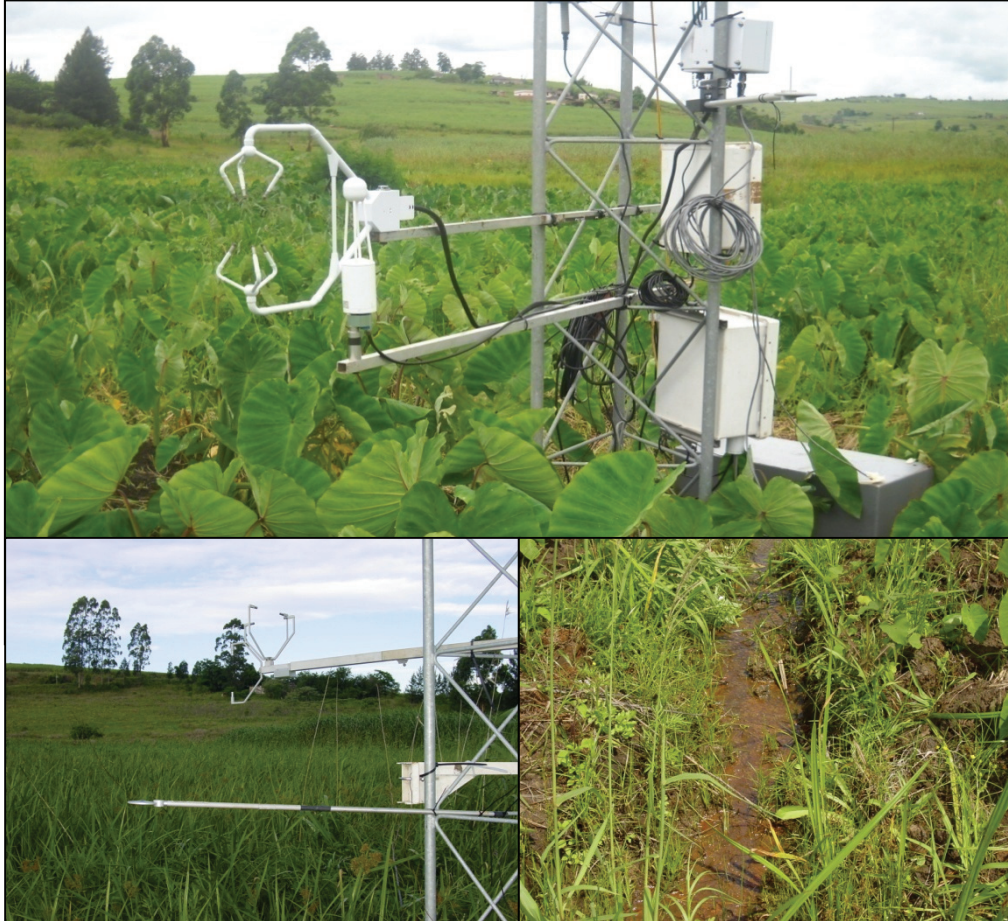


The impact of madumbe (*Colocasia esculenta*) cultivation
on the evaporation of a *Cyperus latifolius* marsh
in KwaZulu-Natal



REPORT TO THE WATER RESEARCH COMMISSION BY

by

Colin Everson and Michael Mengistu

School of Bioresources Engineering and Environmental Hydrology.

Univesity of KwaZulu-Natal

WRC Report No. KV 260/10
ISBN 978-1-4312-0071-9

February 2011

Obtainable from

Water Research Commission
Private Bag X03
Gezina, 0031

orders@wrc.org.za

The publication of this report emanates from a project titled *The impact of madumbe (Colocasia esculenta) cultivation on the evaporation of a Cyperus latifolius marsh in KwaZulu-Natal* (WRC Project No. K8/905).

DISCLAIMER

This report has been reviewed by the Water Research Commission (WRC) and approved for publication. Approval does not signify that the contents necessarily reflect the views and policies of the WRC, nor does mention of trade names or commercial products constitute endorsement or recommendation for use.

TABLE OF CONTENTS

1	INTRODUCTION	1
2	OBJECTIVE AND AIMS	4
3	THE RESEARCH SITE	5
4	METHODOLOGY	7
	4.1 Wetland Water Budget.....	7
	4.2 The Evapotranspiration Component	7
	4.3 Theory of Evapotranspiration Estimation Methods	9
	4.3.1 Eddy covariance method	9
	4.3.2 Surface renewal method	10
	4.3.3 Reference evapotranspiration	11
	4.4 Instrumentation for Evapotranspiration Measurements at the Mbongolwane Wetland Catchment.....	13
	4.4.1 Madumbe site	13
	4.4.2 Sedge site.....	13
	4.4.3 Sugarcane site.....	15
	4.5 Footprint of Surface Layer Flux Measurements	17
5	RESULTS.....	20
	5.1 General Climatic Variables	20
	5.2 Energy Balance Measurements	21
	5.2.1 First field campaign (20 to 26 November 2009)	21
	5.2.2 Second field campaign (8 to 15 January 2010)	23
	5.3 Total Evaporation.....	26
	5.3.1 First field campaign (20 to 26 November 2009)	26
	5.3.2 Second field campaign (8 to 15 January 2010)	27
	5.4 Footprint of Measurements	28
	5.5 Water Use of Madumbes Using FAO-56 Penman-Monteith Model and Crop Factor.....	32
6	CONCLUSION	35
7	REFERENCES	36

LIST OF FIGURES

Figure 3.1	The Mbongolwane wetland catchment with sugarcane in the foreground and the sedge wetland in the background (KwaZulu-Natal).....	5
Figure 3.2	The location of the research site at Mbongolwane within South Africa where evapotranspiration was measured.....	6
Figure 4.1	An extended open path (CSAT 3) eddy covariance system installed on a lattice mast above the madumbe canopy.....	14
Figure 4.2	An Applied Technologies, Inc. (ATI) sonic anemometer mounted on a lattice mast above the sedge.....	15
Figure 4.3	Two SR arms with fine-wire thermocouples mounted on a weather station mast above the sugarcane canopy.....	16
Figure 5.1	Diurnal variations of half-hourly net radiation (R_n), CSAT3 sonic anemometer sensible heat flux estimates (H), and the soil heat flux density (G) at the madumbe site for November 2009.....	21
Figure 5.2	Diurnal variations of half-hourly net radiation (R_n), ATI sonic anemometer sensible heat flux estimates (H) and the soil heat flux density (G) at the sedge site for November 2009.....	22
Figure 5.3	Diurnal variations of half-hourly net radiation (R_n), surface renewal (SR) sensible heat flux estimates (H), and the soil heat flux density (G) at the sugarcane site for November 2009.....	23
Figure 5.4	Diurnal variations of half-hourly net radiation (R_n), CSAT3 sonic anemometer sensible heat flux estimates (H_s) and the soil heat flux density (G) at the madumbe site for January 2010.....	24
Figure 5.5	Diurnal variations of half-hourly net radiation (R_n), ATI sonic anemometer sensible heat flux estimates (H) and the soil heat flux density (G) at the sedge site for January 2010.....	25
Figure 5.6	Diurnal variations of half-hourly net radiation (R_n), surface renewal (SR) sensible heat flux estimates (H), and the soil heat flux density (G) at the sugarcane site for January 2010.....	25
Figure 5.7	The daily total evaporation estimates at the madumbe, sedge, sugarcane sites and reference evapotranspiration (ET_o) (November 2009).....	27
Figure 5.8	The daily total evaporation estimates at the madumbe, sedge, sugarcane sites and reference evapotranspiration (ET_o) (January 2010).....	28
Figure 5.9	The estimated footprint and the peak location of the footprint at midday for four days in November 2009, based on the EC measurements at 1.10 m from the ground surface and horizontal distance x (m) from the measurement position.....	29
Figure 5.10	The cumulative fraction of the measured flux (F) to surface source flux (S_o) ratio and the peak location of the footprint at midday for four days in November 2009.....	30

Figure 5.11	The estimated footprint and the peak location of the footprint at midday for four days in January 2010, based on the EC measurements at 1.30 m from the ground surface and horizontal distance x (m) from the measurement position.....	31
Figure 5.12	The cumulative fraction of the measured flux (F) to surface source flux (S_o) ratio and the peak location of the footprint at midday for four days in January 2010.	32
Figure 5.13	Crop factor (K_c) for the madumbes: (a) November 2009 and (b) January 2010.....	33
Figure 5.14	Daily variation in ET_o (mm), ET estimates from madumbes (using $K_c = 0.6$) and rainfall (mm) for November and December 2009, and January 2010...	34

LIST OF TABLES

Table 5.1	A daily summary of the weather parameters at the Mbongolwane wetland catchment during the first field campaign (20 to 26 November 2009).	20
Table 5.2	A daily summary of the weather parameters at the Mbongolwane wetland catchment during the second field campaign (8 to 14 January 2010).....	20

LIST OF ABBREVIATIONS AND SYMBOLS

Roman

a	amplitude of the air temperature ramps	$^{\circ}\text{C}$
ABL	Atmospheric boundary layer	
ATI	Applied technologies Inc.	
AWS	Automatic weather station	
b_0	Empirical constant	
b_1	Empirical constant	
c_p	Specific heat capacity of air at constant pressure	$\text{J kg}^{-1} \text{ }^{\circ}\text{C}^{-1}$
E	Evaporation	mm
e_a	actual vapour pressure	kPa
E_a	Actual evapotranspiration	mm
E_p	Potential evapotranspiration	mm
e_s	Saturated vapour pressure	kPa
EC	Eddy covariance	
ET_c	Evapotranspiration	mm
ET_o	Reference evapotranspiration	mm
ET	Evapotranspiration	mm
F_s	Vertical turbulent flux	
G	Soil heat flux	W m^{-2}
H	Sensible heat flux	W m^{-2}
LAI	Leaf area index	
OPEC	Open path eddy covariance	
P	Precipitation	mm
Q_g	Discharge to groundwater	mm
Q_s	Discharges at the surface	mm
R_n	Net radiation	W m^{-2}
s	Concentration of specific scalar of interest	ppm
SR	Surface renewal	
T_s	Sonic temperature	$^{\circ}\text{C}$
TDR	Time domain reflectometry	
V_a	wind speed	m s^{-1}
w	Vertical wind speed	m s^{-1}

Greek

α	Weighting factor	
ΔS	Change in soil water storage	mm
λE	Latent energy flux	W m^{-2}
ρ_a	Density of air	kg m^{-3}
τ	Total ramping period	s

1 INTRODUCTION

The madumbe (*Colocasia esculenta*) is known as the ‘potato of the tropics’. It is an important food plant in the hot regions of the world. Madumbes are known by a number of different names – idumbe, taro, cocoyam or dasheen. Madumbes are grown mainly for the underground, easily digestible, starchy tuber. The large elephant-ear-shaped leaves are also used as a type of vegetable. They are regarded as an indigenous plant, although they were thought to have originated from India over 2500 years ago. It is one of the most widely grown traditional crops in Mpumalanga and KwaZulu-Natal, as well as in areas of the Eastern Cape, and Limpopo provinces. The madumbe has a high soil water requirement and, under low rainfall conditions, farmers are very dependent on wetlands for madumbe cultivation.

A key component of the water budget of a wetland is the loss of water to the atmosphere (also called evapotranspiration), which may be strongly affected by the particular vegetation growing in the wetland. To date, very little research has been conducted on the evapotranspiration of different wetland vegetation types occurring in South Africa, except in a few vegetation types (e.g. *Phragmites mauritianus* stands and swamp forests). Further studies on other wetland vegetation types commonly occurring in South Africa are therefore extremely valuable. *Cyperus latifolius* marsh is one of the wetland vegetation types occurring most extensively in KwaZulu-Natal, the Pondoland region of the Eastern Cape Province and in the Mpumalanga and Limpopo provinces. *C. latifolius* is a sedge with a C4 photosynthetic pathway, which is generally an adaptation for water-stressed conditions. This suggests that it may have a higher water use efficiency than C3 plants such as *Phragmites mauritianus* and swamp forest trees. Madumbes have a high tolerance to water logging and are often cultivated in *C. latifolius* marshes. In assessing the potential impact of madumbe cultivation on wetlands, an important knowledge gap is the water loss from madumbes to the atmosphere, for which no studies have been undertaken in South Africa or elsewhere. For modelling these water losses using hydrological models it is useful to have accurately determined crop coefficients. To date no crop coefficients have been determined for madumbes.

The South African Sugar Research Institute have recently initiated long-term monitoring of the effects of different sugarcane management practices on runoff in the catchment of the Mbongolwane wetland, a large wetland near Eshowe, KwaZulu-Natal. The Mbongolwane wetland (approximately 3 ha) supports major stands of *C. latifolius* as well as extensive madumbe cultivation in the *C. latifolius* wetlands. Currently, the hydrological monitoring at Mbongolwane is confined to the catchment upslope of the wetland. Research on the effect of madumbe cultivation on the vegetation composition and geomorphology of the Mbongolwane wetland has already been undertaken (Kotze, *et al.*, 2002); however no research on the hydrology of the wetland exists. This is recognised as an important gap. Thus, it is suggested that a study on the evapotranspiration of *C. latifolius* and madumbe areas, together with monitoring of the water table in the wetland, would not only provide results that would be useful points of reference at a national and international level, but would also contribute valuable information to the integrated management of the Mbongolwane wetland and many other wetlands used in a similar way. If restricted to the less sensitive parts of the wetland, madumbe cultivation is reported to do little harm to the wetland. This is provided that pesticides and artificial fertilisers are not used, tillage is by hand and large-scale drainage and cultivation is not applied. However, the impact of madumbe cultivation on the wetland water budget has never been quantified in order to justify this claim. In addition, there are now plans by Woolworths to commercialise the cultivation of madumbe. The Woolworths project is part of a far-reaching empowerment scheme to support over 200 traditional subsistence farmers in KwaZulu-Natal to develop organic food production with organically-grown madumbes. The Woolworths-supported scheme opens up opportunities for previously disadvantaged South African farmers to enter and participate in the economic mainstream. However, the extensive cultivation of madumbe for commercial gain may have previously unrecognised negative impacts on the *C. latifolius* wetlands which, in turn, may affect the sustainability of this venture.

Evapotranspiration (*ET*) remains the significant uncertainty in any water budgeting of ecosystems. Since wetlands in arid or seasonally arid areas of temperate and tropical regions have warm growing seasons, wetlands may be subjected to a significant influence of both air and water advection. Consequently, *ET* likely comprises the largest loss from the wetland water budget (Drexler *et al.*, 2008). Therefore, accurate determination of evaporation has consequences, not only for monitoring the impact of madumbe cultivation, but also for the

management of river flows and water resources at a catchment scale.

A prerequisite to managing water in ‘water scarce regions,’ is the accurate representation of water distribution. A precise determination of water budgets for catchments and their hydrological response units is paramount. Wetlands have a naturally defined hydrological response in catchment processes. Their health, therefore, impacts the quantity, persistence and variability of catchment discharge, although their precise function in different catchment positions is still to be suitably determined (e.g. Bullock and Acreman, 2003). Thus, when dealing with an impacted, restored or natural wetland it is necessary to comprehensively determine their water budgets in order to understand the functioning of the system and then to set appropriate management guidelines. This is particularly pertinent in the context of anticipated climate and land use changes.

With the advent of techniques to accurately quantify *ET* from terrestrial and aquatic surfaces, the calibration of the traditional *ET* models for local conditions becomes possible, ultimately improving the reliability of the mass balances (e.g. water or nutrient budgets) derived for the systems in question.

This WRC-funded project (K8/905) focused on the impact of madumbe cultivation on the evaporation of a *Cyperus latifolius* marsh within the Mbongolwane wetland catchment.

2 AIMS AND OBJECTIVES

This report describes two field campaigns made in the madumbe growing season (November 2009) and summer (January 2010). The aim of the project was to quantify the water use of three vegetation types: madumbe (*Colocasia esculenta*); sedge (*Cyperus latifolius*) wetland; and sugarcane (*Acer Saccharum*) in the Mbongolwane wetland catchment. Specific objectives were:

1. Accurate quantification of actual *ET* losses from sedge-madumbe wetland cultivation systems in order to provide critical information of the systems mass balance;
2. Determination of seasonal trends in *ET* losses and their proportional loss from the wetland mass balance;
3. Differentiating actual *ET* losses of the wetland from those of their contributing catchment and
4. Calibration of empirical meteorological *ET* models to local conditions using model efficiency criteria.

3 THE RESEARCH SITE

The Mbongolwane wetland catchment is located in northern KwaZulu-Natal, about 20 km S-W of Eshowe (Figure 3.1 and 3.2).



Figure 3.1. The Mbongolwane wetland catchment with sugarcane in the foreground and the sedge wetland in the background (KwaZulu-Natal).

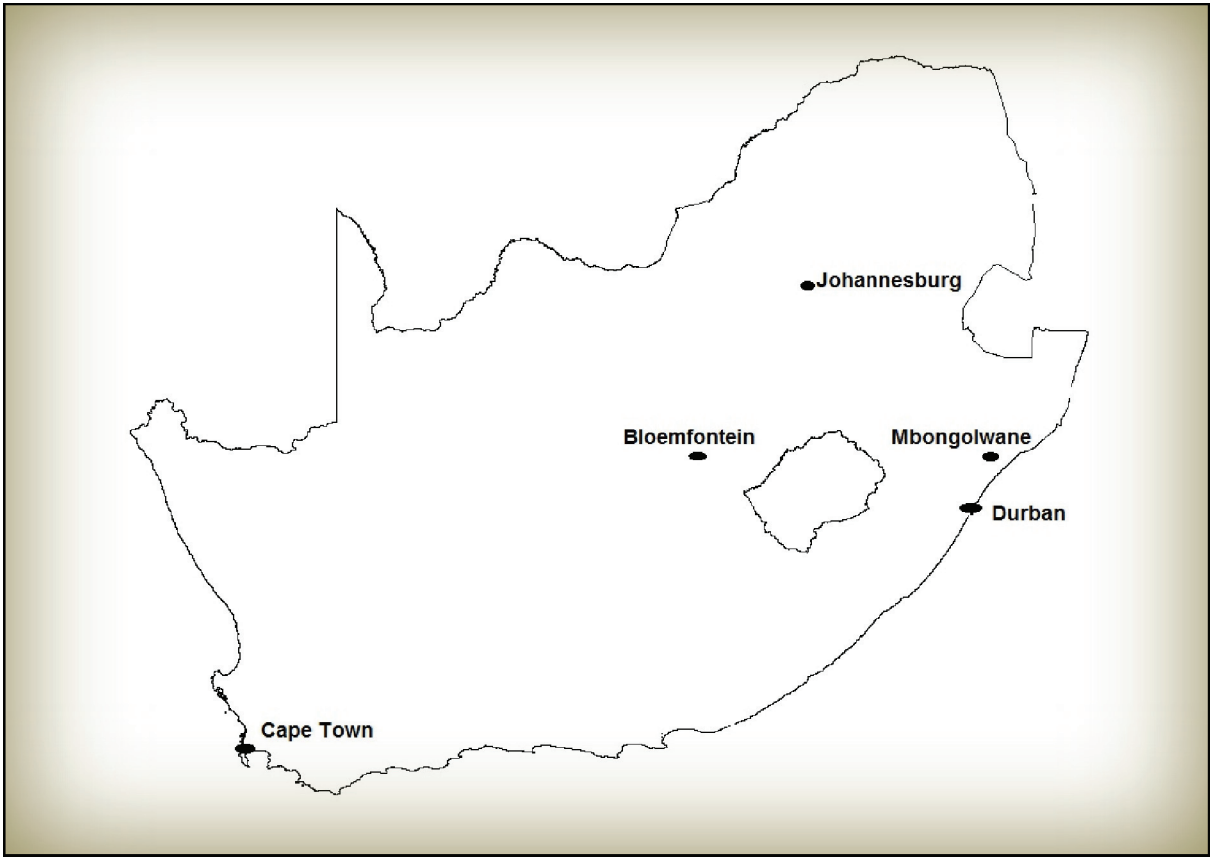


Figure 3.2. The location of the research site at Mbongolwane within South Africa where evapotranspiration was measured.

4 METHODOLOGY

4.1 Wetland Water Budget

The wetland water budget is the result of both inflows to the wetland (from surface and subsurface sources) as well as precipitation. The residual storage of the system results from the losses to outflows in the surface and subsurface as well as ET (Eq. 1), such that:

$$ET = P - \Delta S - Q_s - Q_g \quad (1)$$

where ET is evapotranspiration; P is precipitation; ΔS is change in soil water storage; and Q_s and Q_g are discharges at the surface and to groundwater, respectively.

There is a general lack of understanding of wetland hydrological processes in arid and semi-arid areas (Drexler *et al.*, 2008) whilst it is noted that suitable studies of wetland hydrology are lacking in South Africa (Grenfell *et al.*, 2005). Meanwhile, only a few studies have been conducted on wetland hydrology in the greater Southern African region (e.g. Bullock, 1992, McCartney, 2000); however, these have for the most part, focused on wetlands in the high altitude interior of the sub-continent. The absence of the rigorous determination of ET in most cases highlights the uncertainty of water budgets that are developed for these systems.

4.2 The Evapotranspiration Component

Dalton's Law (c. 1802) is a law of partial pressures governing the total pressure of a gas mixture as the sum of the pressures of the individual component gases. This law describes the main driving force of evaporation as being the vapour pressure deficit, whereby the rate of evaporation is a function of the difference between the ability of the air to hold water (based on air temperature and relative humidity) and the energy in the water (function of temperature) to make it give up water to the air (Ward and Trimble, 2004). This is formulated by Dingman (2002) as: Dalton's Law: $E = (b_0 + b_1 * v_a) * (e_s - e_a)$ where E is the rate of evaporation; b_0 and b_1 are empirical constants, depending on the measuring height of wind

speed and air vapour pressure, respectively; v_a is wind speed; e_s is the saturated vapour pressures of the evaporating surface; and e_a is the vapour pressure of the overlying air (Dingman, 2002).

In well-watered ecosystems actual evapotranspiration (ET_a) occurs at the potential rate (ET_p) and is limited only by available energy (Jacobs *et al.*, 2002). Jacobs *et al.* (2002) characterised this as first-stage evapotranspiration ($ET_a \approx ET_p$), which is typical in wetlands when they are inundated. When the water table drops below the shallow root zone during drying phases, water becomes limited and the wetland vegetation becomes stressed so second-stage evapotranspiration occurs ($ET_a < ET_p$). Thus the seasonal nature of precipitation in eastern South Africa will likely create a marked two-stage ET regime, of which the second stage ET will be linked to the plant available water function (PAW) of different soil types, with high ET rates in summer and low ET rates in winter. While ET_p can be calculated relatively easily, determination of actual evapotranspiration (ET_a) requires detailed measurement. Since ET_a is so important to the water budget, it warrants a full analysis to understand the contribution of complex surface types, vegetation communities and hydrological conditions to evapotranspiration losses.

Traditional estimates of wetland ET using meteorologically based models can be highly variable with large degrees of error and have utility only during certain periods of the year (Drexler *et al.*, 2004). For instance, the discrepancy between the traditional ET models compared to energy balance and Class A-pan evaporation techniques was observed in the hydrological modelling of the Nylsvlei floodplain (Birkhead *et al.*, 2007). These anomalies have been similarly observed for freshwater marsh ET when compared to the eddy covariance technique (Sun and Song, 2008). Models that incorporate a crop coefficient for ET have also been found to be inefficient since the ET rates for the crop (e.g. *Phragmites australis*, common reed) have been found to vary considerably by region and climatic conditions (Allen *et al.*, 1998; Fermor *et al.*, 2001). Furthermore, errors can be introduced into these traditional models where there is no accounting for different functional groups of vegetation which have different rates of water conductance, thereby exerting various controls over ET (Koerselman and Beltman, 1988; Lafleur, 1990 as cited by Drexler *et al.*, 2004). Additional influence is generated by the very shape and geographical extent of a wetland. Wetlands tend to have higher ET rates when they are surrounded by areas with low ET , such as degraded grassland,

than if surrounded by areas with higher rates of ET , such as forests (i.e. the oasis effect). Also, the extent and orientation of a wetland plays a part since wetlands such as riparian zones and marsh fringes around lakes tend to have higher rates of ET than large expanses of wetlands with a greater area-to-perimeter ratio (i.e. the clothes line effect) (Linacre, 1976 as cited by Drexler *et al.*, 2004).

The essential challenge, therefore, for these meteorologically-based estimates of wetland ET is to adequately differentiate energy balances in heterogeneous patches of vegetation, open water and bare soil with varying micro-topography and surface roughness, such as between a wetland and its contributing catchment. Direct measures of ET , such as eddy covariance, scintillometry and surface renewal, now provide a means of accounting for these variations that the models overlook. Direct measures of ET are ultimately based on the shortened energy balance equation (Eq. 2):

$$R_n = G + H + \lambda E \quad (2)$$

where R_n is net radiation; G is heat flux transfer to/from soil and water; H is the sensible heat flux density; and λE is the latent heat flux.

4.3 Theory of Evapotranspiration Estimation Methods

4.3.1 Eddy covariance method

In fully turbulent flow, the mean vertical fluxes of heat, water vapour and momentum can be defined directly in terms of the turbulent (eddy) components of vertical velocities and of the properties being transferred (Rosenberg *et al.*, 1983; Kaimal and Finnigan, 1994). Mean flux across any plane implies covariance between the wind component normal to that plane and the scalar entity of interest (Kaimal and Finnigan, 1994; Arya, 2001).

The eddy covariance (EC) method provides a direct measure of the vertical turbulent flux of a scalar entity of interest (F_s) across the mean horizontal stream lines (Swinbank, 1951), provided that fast response sensors (≈ 10 Hz) for the wind vector and scalar entity of interest

are available (Meyers and Baldocchi, 2005). For a sufficiently long averaging period of time over horizontally homogeneous surface, the flux is expressed as:

$$F_s = \rho_a \overline{w's'} \quad (3)$$

where F_s is the vertical turbulent flux, ρ_a the density of air; w is the vertical wind speed; and s is the concentration of the scalar of interest. The primes in Eq. (3) indicate fluctuation from a temporal average (i.e. $w' = w - \bar{w}$; $s' = s - \bar{s}$) and the over bar represents a time average. The vertical wind component is responsible for the flux across a plane above a horizontal surface. Based on Eq. (3), the sensible heat flux H can be expressed as:

$$H = \rho_a c_p \overline{w'T_s'} \quad (4)$$

where c_p is the specific heat capacity of air; w' denotes the fluctuation from the mean of the vertical wind speed; and T_s' is the fluctuation of air temperature from the mean. The averaging period of the instantaneous fluctuations of w' and s' should be long enough (30 to 60 minutes) to capture all of the eddy motions that contribute to the flux (Meyers and Baldocchi, 2005).

4.3.2 Surface renewal method

The surface renewal (SR) method is a simple and relatively inexpensive technique that is based on the principle that an air parcel near the surface is renewed by an air parcel from above (Paw U *et al.*, 1995). This process involves ramp-like structures (rapid increase and decrease of a scalar), which are the result of turbulent coherent structures that are known to exhibit ejections and sweeps under shear conditions (Gao *et al.*, 1989; Raupach *et al.*, 1989; Paw U *et al.*, 1992). The theory of heat exchange between a surface and the atmosphere using the SR method is described in detail in Paw U *et al.* (1995), Snyder *et al.*, (1996) and Paw U *et al.* (2005). The exchange of heat energy between a surface and the atmosphere is expressed as:

$$H = \alpha \rho_a c_p z \frac{a}{\tau} \quad (5)$$

where α is a weighting factor; a is amplitude of the air temperature ramps; and τ is the total ramping period. The amplitude (a) and the ramping period (τ) were deduced using analytical solutions of Van Atta (1977) for air temperature structure function:

$$S^n(r) = \frac{1}{m-j} \sum_{i=1+j}^m (T_i - T_{i-j})^n \quad (6)$$

where n is the power of the function; m is the number of data points in the time interval measured at frequency f (Hz); j is the sample lag between data points corresponding to a time lag $r = j/f$; and T_i is the i th temperature sample. Time lags of 0.5 and 1.0 s were used in this study. Second, third and fifth order of the air temperature structure parameter are required to solve for a and τ .

The sensible heat flux was finally estimated from Eq. (5) using the measurement height (z) and a weighting factor (α) obtained by calibration using the EC method. The weighting factor (α) depends on the measurement height, canopy architecture and thermocouple size (Snyder *et al.*, 1996; Spano *et al.*, 1997, 2000). Once determined, it is fairly stable and does not change from site to site, regardless of weather conditions, unless the surface roughness changes (Snyder *et al.*, 1996; Spano *et al.*, 2000; Paw U *et al.*, 2005).

4.3.3 Reference evapotranspiration

A number of empirical and semi-empirical methods have been developed over the last five decades by a collection of scientists to estimate evapotranspiration from different climatic variables. The FAO-56 Penman-Monteith method was considered to offer the best results with minimum possible error in relation to a living grass reference crop (Allen *et al.*, 1998). The FAO-56 Penman-Monteith method defines the reference crop as “a hypothetical crop with an assumed height of 0.12 m having a surface resistance of 70 m s^{-1} and a reflection coefficient of 0.23, closely resembling the evaporation of an extensive surface of green alfalfa grass of uniform height, actively growing and adequately watered” (Allen *et al.*, 1998). By further assuming a constant psychrometric constant (γ), simplifying the air density (ρ_a) using a surface resistance of 70 m s^{-1} and estimating aerodynamic resistance from an inverse function of wind speed, the FAO-56 equation can be expressed as:

$$\lambda ET = \frac{0.408\Delta(R_n - F_s) + \gamma \frac{900}{T + 273} U_2 (e_s - e_a)}{\Delta + \gamma(1 + 0.34U_2)} \quad (7)$$

where T is the mean air temperature ($^{\circ}\text{C}$) at a height of 2 m, U_2 is the mean wind speed (m s^{-1}) at a height of 2 m and Δ is the slope of the saturation-vapour pressure versus temperature curve.

The equation uses standard weather station data including solar radiation, air temperature, relative humidity and wind speed. All sensors should be mounted at a height of 2 m above an extensive surface of green grass shading the ground and not short of water (Allen *et al.*, 1998).

The FAO-56 Penman-Monteith equation is a representation of the physical and physiological factors controlling the evaporation process. By using the FAO-56 Penman-Monteith definition for reference evapotranspiration (ET_o), it is possible to calculate crop coefficients (K_c) by relating the measured evapotranspiration (ET_c) to the calculated ET_o :

$$K_c = \frac{ET_c}{ET_o} \quad (8)$$

Allen *et al.* (1998) describe how the equation can be re-arranged to calculate crop evapotranspiration if ET_o is calculated from weather data and K_c is known. The crop coefficient is defined for different crops and in most cases a dual crop coefficient is used to represent two stages in the growth of a crop. Allen *et al.* (1998) provide details on the different crop coefficients suggested for different crops and the possible adjustments that can be made. The equation can be applied for monthly, ten-day, daily and even hourly time-steps, depending on the availability of the data.

4.4 Instrumentation for Evapotranspiration Measurements at the Mbongolwane Wetland Catchment

4.4.1 Madumbe site

An extended open path eddy covariance (OPEC) system (Campbell Scientific Inc., Logan, Utah, USA) was used as an eddy covariance system to measure fluxes of water vapour and carbon dioxide (Figure 4.1). The OPEC system consists of a CR5000 datalogger, a CSAT3 three-dimensional sonic anemometer, a LI-7500 open path infrared gas analyser (IRGA), a HMP45C temperature and humidity probe and energy balance sensors consisting of NR-LITE net radiometer, two soil heat flux plates, one soil temperature averaging probe and one CS616 soil moisture reflectometer. The system measures carbon dioxide flux, latent energy flux, momentum flux, a computed sensible heat flux, net radiation, a computed soil heat flux density, temperature, humidity, horizontal wind speed and wind direction.

The OPEC system was installed on a lattice mast at 1.10 m (November 2009) and 1.30 m (January 2010) above the soil surface for the two window periods of measurement. The average height of the madumbes was 0.60 m (November 2009) and 0.80 m (January 2010). The average leaf area index (LAI) of the madumbes measured using a LAI-2000 (LI-COR Inc, Lincoln, Nebraska, USA) was $1.17 \text{ m}^2 \text{ m}^{-2}$.

4.4.2 Sedge site

An Applied Technologies, Inc. (ATI) sonic anemometer (“Sx” style probe) was used as an eddy covariance system to measure three dimensional wind velocity components by transmitting and receiving sonic signals along fixed orthogonal directions and sensible heat flux density at 2.10 m above the soil surface. The sonic anemometer was mounted on a lattice mast located in the middle of the plot (Figure 4.2), and was connected to a CR3000 datalogger (Campbell Scientific Inc., Logan, Utah, USA). All eddy covariance data were sampled at a frequency of 10 Hz and data were processed online in the datalogger. The high frequency data, the two-minute and thirty-minute averages of the covariances between wind speed (u , v and w), sonic temperature (T_s) and wind direction were calculated and stored for further analysis.



Figure 4.1. An extended open path (CSAT 3) eddy covariance system installed on a lattice mast above the madumbe canopy.

The average canopy height of the sedge was 1.45 m (November 2009) and 1.60 m (January 2010). The average leaf area index of the sedge measured using a LAI-2000 (LI-COR Inc, Lincoln, Nebraska, USA) was $1.36 \text{ m}^2 \text{ m}^{-2}$.

Additional sensors for measuring the remaining energy balance components were also used. Net irradiance was measured using a NR-LITE net radiometer (Kipp and Zonen, Delft, The Netherlands) at 2.0 m above the ground. The soil heat flux was also measured using two soil heat flux plates (HFT-S, REBS, Seattle, WA) placed at a depth of 80 mm below the soil surface. A system of parallel thermocouples at depths of 20 and 60 mm were used for measuring the soil heat stored above the soil heat flux plates. Volumetric soil water content in the first 60 mm was also measured using a CS615 time domain reflectometer (TDR). The measurements were sampled every 10 s with a Campbell CR23X and 30-minute averages were computed.



Figure 4.2. An Applied Technologies, Inc. (ATI) sonic anemometer mounted on a lattice mast above the sedge.

4.4.3 Sugarcane site

The surface renewal (SR) method was used to estimate sensible heat flux density (Figure 4.3). The SR technique is based on high frequency air temperature measurements. Air temperature was measured using two unshielded type-E fine-wire thermocouples (75 μm diameter) placed at heights of 1.65 and 2.00 m (November 2009) and at 2.30 and 2.60 m above the ground surface in January 2010. The fine wire thermocouples were connected to a CR1000 datalogger (Campbell Scientific Inc., Logan, Utah, USA). Air temperature data were sampled at a frequency of 10 Hz and then lagged by 0.4 s and 0.8 s. The second, third and fifth air temperature structure function values required by the Van Atta (1977) approach were then formed after lagging the air temperature data by specified amounts – either by 0.4 and 0.8 s. The data were then averaged and stored every two minutes in the datalogger.

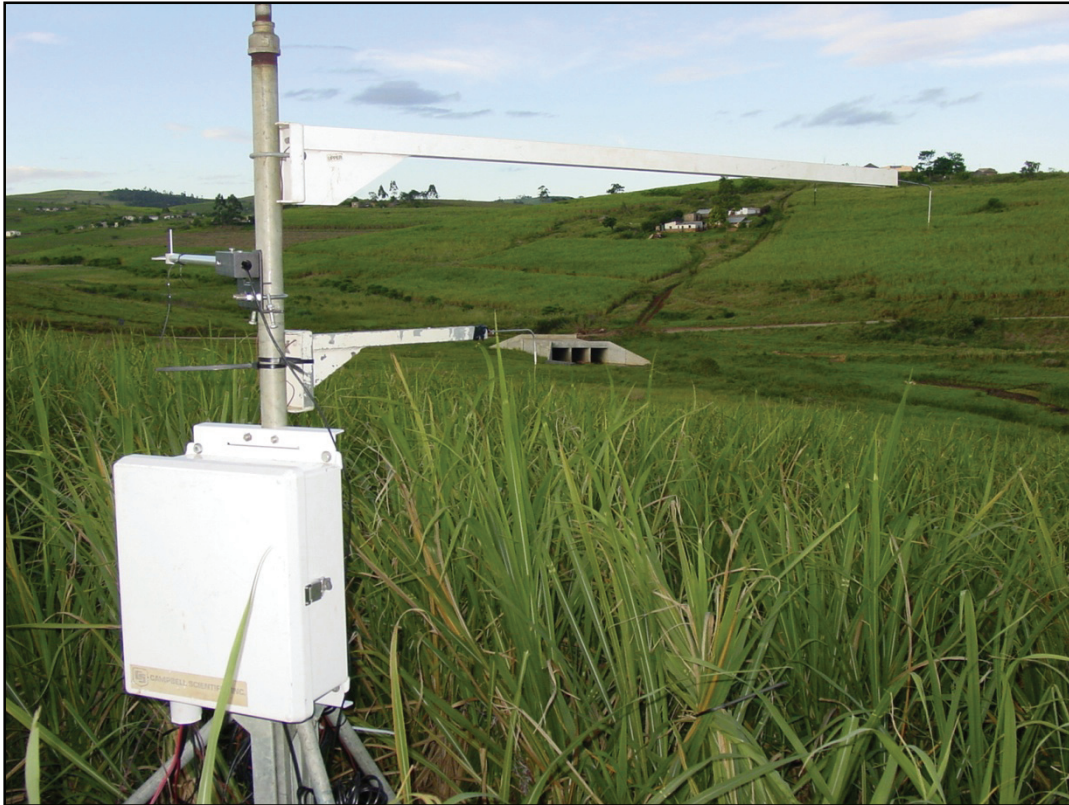


Figure 4.3. Two SR arms with fine-wire thermocouples mounted on a weather station mast above the sugarcane canopy.

Additional measurements included the remaining components of the energy balance. Net irradiance was measured using a net radiometer (Model 240-110 NR-Lite, Kipp and Zonen, Delft, The Netherlands) placed at 2.20 m above the ground surface. Two soil heat flux plates (model HFT-S, REBS) were used to measure soil heat flux density at a depth of 80 mm and a system of parallel-thermocouples at depths of 20 and 60 mm were used to calculate the heat stored above the plates. Volumetric soil water content in the first 60 mm of the soil surface was measured using a time domain reflectometer (CS615, Campbell Scientific Inc., Logan, Utah, USA). The sensors were connected to a CR23X datalogger with measurements every ten seconds and averages obtained every thirty minutes.

The average canopy height of the sugarcane was 1.65 m (November 2009) and 2.0 m in January 2010. The average leaf area index (LAI) of the sedge measured using a LAI-2000 (LI-COR Inc, Lincoln, Nebraska, USA) was $2.77 \text{ m}^2 \text{ m}^{-2}$.

4.5 Footprint of Surface Layer Flux Measurements

Understanding the turbulent transport of surface layer fluxes from natural and vegetated surfaces is very important in land-atmosphere interaction studies in the atmospheric boundary layer (ABL). Turbulent flux sensors are deployed to measure signals that reflect the influence of the underlying surface on the turbulent exchange (Schmid, 2002). Surface layer flux measurements are influenced by diffused fluxes upwind of the surface under study, which may include large areas with different types of sources and sinks (Gash, 1986).

This spatial context of the measurement of surface layer fluxes is commonly referred to as the footprint of a measurement (Schmid, 2002), or the effective fetch (Pasquill, 1972, cited by Schmid, 2002). The footprint of a turbulent flux measurement defines the spatial context of the measurement or the ‘field of view’ of the measurement of the surface-atmosphere exchange (Schmid, 2002). The estimation of the footprint of sensible and latent heat fluxes is therefore important in the field of micrometeorology and mainly depends on the measurement height, surface roughness and atmospheric stability (Gash, 1986; Leclerc and Thurtell, 1990; Savage *et al.*, 1997; Hsieh *et al.*, 2000). The footprint function is mathematically defined by relating the measured flux $F(x, z_m - d)$ at a distance (x) from the source (at a measurement height z_m and for a surface with a zero displacement height, d) to the spatial distribution of the surface flux (Horst and Weil, 1992):

$$F(x, z_m - d) = \int_{-\infty}^x S(x) f(x, z_m - d) dx \quad (9)$$

where $F(x, z_m - d)$ is the flux measured at height $z_m - d$; $S(x)$ the source strength at a distance x ; f the footprint at a distance x (with distance x taken as the downwind fetch).

Hsieh *et al.* (2000) developed an analytical footprint model based on a combination of Lagrangian stochastic dispersion model results and dimensional analysis. The footprint function (f) for a length scale (z_u) in this study is defined as (Hsieh *et al.*, 2000):

$$f(x, z_m - d) = \frac{1}{k^2 x^2} D z_u^P |L_o|^{1-P} \exp\left(\frac{-1}{k^2 x} D z_u^P |L_o|^{1-P}\right) \quad (10)$$

where k ($= 0.4$) is the von Karman's constant; x the downwind fetch distance; L_o the Monin-Obukhov length; and D and P similarity constants, obtained by Hsieh *et al.* (2000) and expressed for different atmospheric stability conditions as:

$D = 0.28$ and $P = 0.59$ for unstable conditions;

$D = 0.97$ and $P = 1$ for near neutral and neutral conditions; and

$D = 2.44$ and $P = 1.33$ for stable conditions.

The length scale (z_u) expressed by Hsieh *et al.* (2000) and extended for a surface with a displacement height (d) and surface roughness length (z_o) (Savage *et al.*, 2004), which is only valid for $z_m > d + z_o$, is defined as:

$$z_u = (z_m - d) \cdot \frac{z_m - d}{z_m - (d + z_o)} \cdot \left[\ln \frac{z_m - d}{z_o} - 1 + \frac{z_o}{z_m - d} \right] \quad (11)$$

The cumulative fraction of the flux (F) to surface source flux (S_o) ratio at distance x from the source and at an effective height of $z_m - d$ from the ground surface can be estimated using (Hsieh *et al.*, 2000):

$$\frac{F(x, z_m - d)}{S_o} = \exp\left(\frac{-1}{k^2 x} D z_u^P |L_o|^{1-P}\right) \quad (12)$$

and the peak location of the footprint (x_{peak}) m can be calculated as:

$$x_{peak} = \frac{D z_u^P |L_o|^{1-P}}{2 k^2} \quad (13)$$

The main advantage of the Hsieh *et al.* (2000) model is its ability to analytically relate atmospheric stability, measurement height and surface roughness length to flux and footprint.

Flux footprint analysis is commonly used to quantify the contributing source areas to scalar flux measurement or to examine adequate fetch requirements (Hsieh *et al.*, 2000). As a ‘rule of thumb’ the fetch-to-height ratio is 100 to 1. Over a homogeneous surface, the exact location of a sensor is not an issue because the fluxes from all parts of the surface are assumed equal (Schmid, 2002). However, for a heterogeneous surface the measured signal depends on which part of the surface has the strongest influence on the sensor and thus on the location and size of its footprint (Schmid, 2002). Therefore, turbulent flux sensors must be located sufficiently high so that the footprint of the flux measurement covers a representative sample of the surface being studied throughout the range of atmospheric conditions encountered at the site (Finnigan, 2004).

5 RESULTS

5.1 General Climatic Variables

The weather conditions at the site for both field campaigns are presented in Tables 1 and 2, respectively. Air temperature fluctuated diurnally with a minimum of 11.4 °C at night and a maximum of 34.0 °C during the day (Table 5.1). The mean wind speed for both field campaigns was 2.5 m s⁻¹. The prevailing wind directions at the site were between 100° and 180°, representative of S-E winds (Tables 5.1 and 5.2). The site is characterised by humid weather conditions with the minimum relative humidity of 35% during the measurement periods.

Table 5.1. A daily summary of the weather parameters at the Mbongolwane wetland catchment during the first field campaign (20 to 26 November 2009).

Date	Solar rad. (MJ m ⁻²)	Wind speed (m s ⁻¹)	Wind direction (°)	Air Temperature (°C)			RH (%)		Rain (mm)
				max	min	mean	max	min	
20/11/2009	6.6	2.7	182	18.4	11.4	14.0	97.3	78.8	13.5
21/11/2009	10.9	1.8	156	18.2	11.9	14.3	97.5	68.3	7.0
22/11/2009	24.5	3.3	122	25.0	12.9	18.4	96.5	38.8	0.3
23/11/2009	27.6	2.5	187	27.7	13.1	20.9	91.7	37.6	0
24/11/2009	16.8	2.0	154	24.7	13.5	18.4	97.2	53.7	0
25/11/2009	23.8	2.1	92	30.4	16.4	22.2	96.6	48.3	0
26/11/2009	25.0	3.1	118	33.7	16.4	25.1	96.6	38.5	0

Table 5.2. A daily summary of the weather parameters at the Mbongolwane wetland catchment during the second field campaign (8 to 14 January 2010).

Date	Solar rad. (MJ m ⁻²)	Wind speed (m s ⁻¹)	Wind direction (°)	Air Temperature (°C)			RH (%)		Rain (mm)
				max	min	mean	max	min	
08/01/2010	17.6	2.3	163	28.1	15.2	21.5	97.0	57.6	0
09/01/2010	18.9	2.1	115	28.5	18.7	22.4	96.6	57.4	10
10/01/2010	24.8	2.2	148	33.6	17.2	20.1	94.0	38.0	0
11/01/2010	16.1	2.1	147	29.0	20.2	19.2	97.0	59.0	0
12/01/2010	26.2	2.3	162	28.7	20.1	20.0	96.0	60.0	0
13/01/2010	14.3	2.5	150	26.3	18.7	21.5	94.7	63.8	0.7
14/01/2010	28.3	2.5	124	34.3	16.4	25.4	96.4	34.7	0

5.2 Energy Balance Measurements

5.2.1 First field campaign (20 to 26 November 2009)

The diurnal course of the daily net radiation was similar at the madumbe, sedge and sugarcane sites (Figures 5.1, 5.2 and 5.3). However, net radiation was 50 to 100 W m^{-2} lower at the madumbe site for some of the days (Figure 5.1). This was due to the lower LAI (not full cover) and differences in albedo compared to the sedge and sugarcane sites with higher LAI values. The maximum daily net radiation varied from 600 to 800 W m^{-2} during the measurement period at the three sites.

The daily maximum soil heat flux densities were between 200 and 300 W m^{-2} at the madumbe and sedge sites for clear days (Figures 5.1 and 5.2), whereas the sugarcane site was between 90 and 110 W m^{-2} (Figure 5.3). These high soil heat flux density values at the madumbe and sedge sites were due to the high volumetric soil water content (>70%) which significantly influenced the heat stored in the soil (the specific heat capacity of water is higher than that of soil) when compared to the sugarcane site with much lower volumetric soil water content (between 35 to 45%).

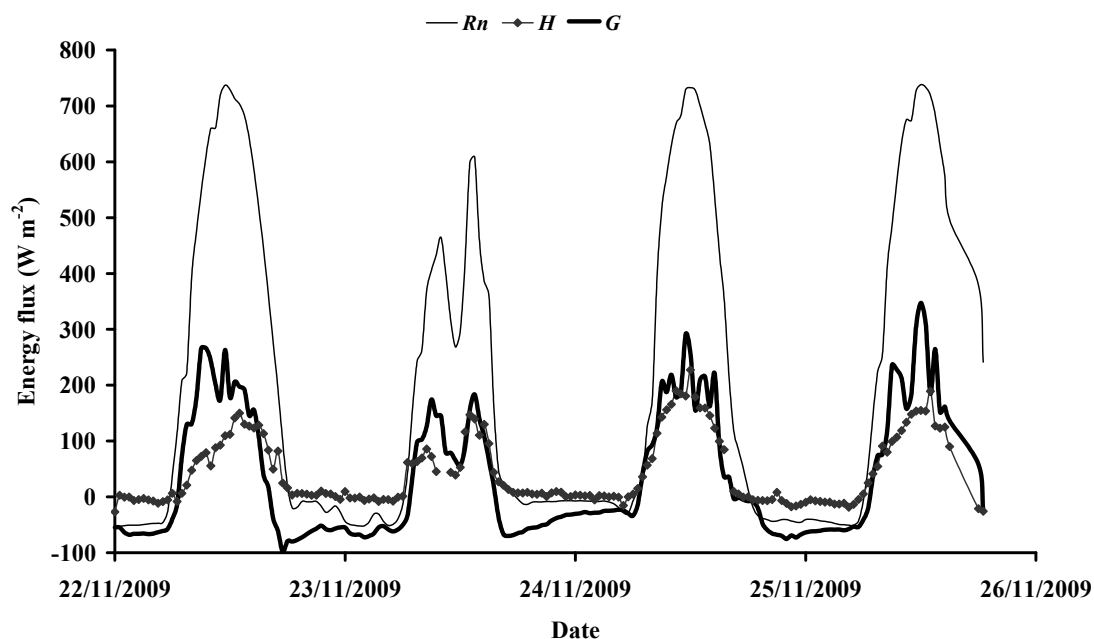


Figure 5.1. Diurnal variations of half-hourly net radiation (R_n), CSAT3 sonic anemometer sensible heat flux estimates (H), and the soil heat flux density (G) at the madumbe site for November 2009.

In addition, the tall and dense full cover canopy of the sugarcane shading the soil surface at the sugarcane site (higher LAI) caused a significantly lower soil heat flux (Figure 5.3) during the day, in contrast to the madumbe and sedge sites.

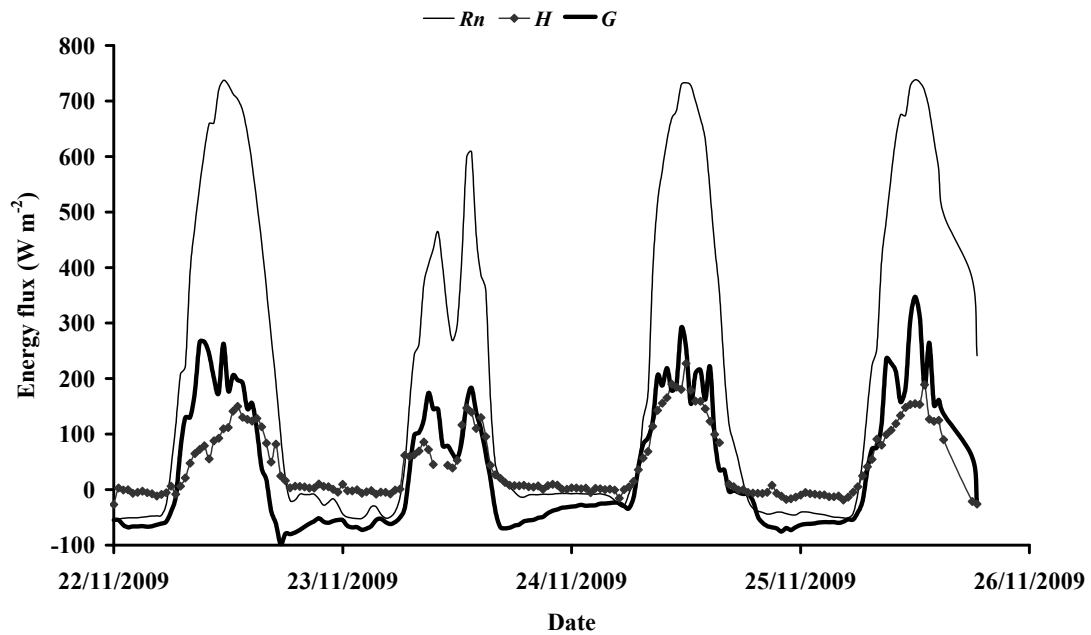


Figure 5.2. Diurnal variations of half-hourly net radiation (R_n), ATI sonic anemometer sensible heat flux estimates (H) and the soil heat flux density (G) at the sedge site for November 2009.

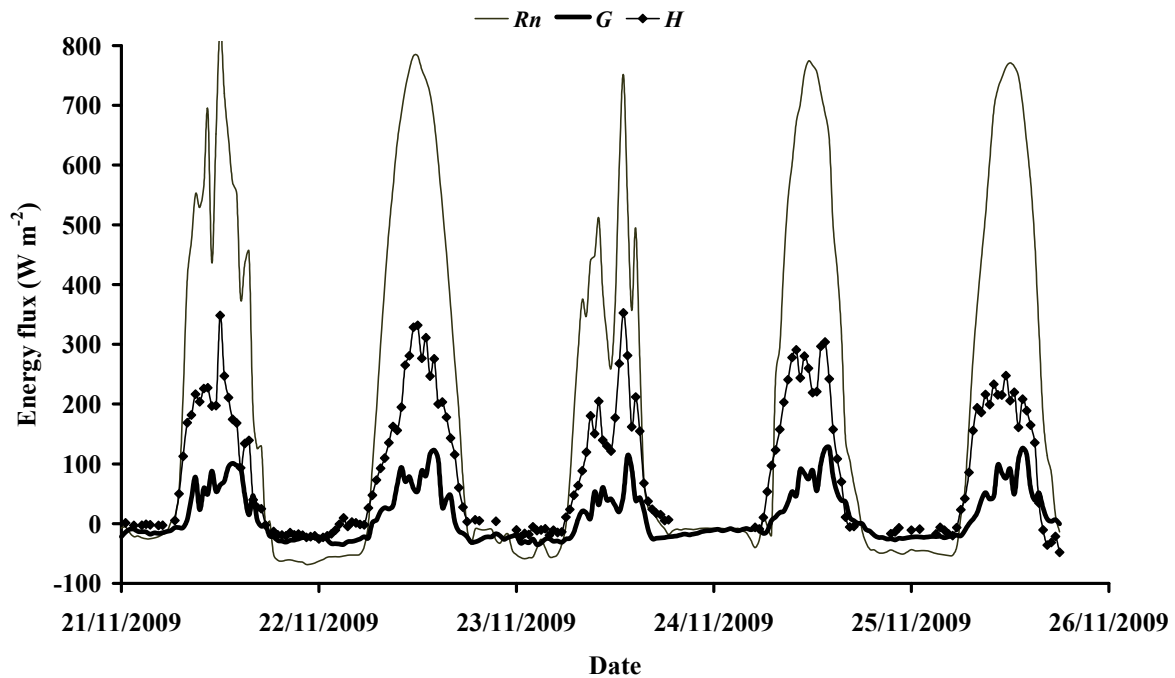


Figure 5.3. Diurnal variations of half-hourly net radiation (R_n), surface renewal (SR) sensible heat flux estimates (H), and the soil heat flux density (G) at the sugarcane site for November 2009.

The sensible heat flux (H) followed the diurnal trend of the net radiation at the three sites. The maximum daily sensible heat flux varied between 150 and 250 W m^{-2} , which was a significant portion of the available energy.

5.2.2 Second field campaign (8 to 15 January 2010)

The diurnal variation of the daily net radiation was similar at the madumbe, sedge and sugarcane sites (Figures 5.4, 5.5 and 5.6). However, the net radiation fluctuated significantly in January 2010 at the three sites due to clouds compared to the first field campaign in November 2009 and the maximum daily net radiation varied from 350 to 750 W m^{-2} during the measurement period at the three sites (Figures 5.1, 5.2 and 5.3).

The soil heat flux at the madumbe site was higher compared to the sedge and the sugarcane sites (Figures 5.4, 5.5 and 5.6). The daily maximum soil heat flux densities were between 100 and 200 W m^{-2} at the madumbe and sedge sites, whereas the sugarcane site was between 50

and 100 W m^{-2} (Figure 5.6). The soil heat flux values at all three sites were lower than those measured during the first field campaign as the soils were drier with lower volumetric soil water contents.

The sensible heat flux (H) followed the diurnal trend of the net radiation at the madumbe, sedge and sugarcane sites. The maximum daily sensible heat flux varied between 50 and 250 W m^{-2} .

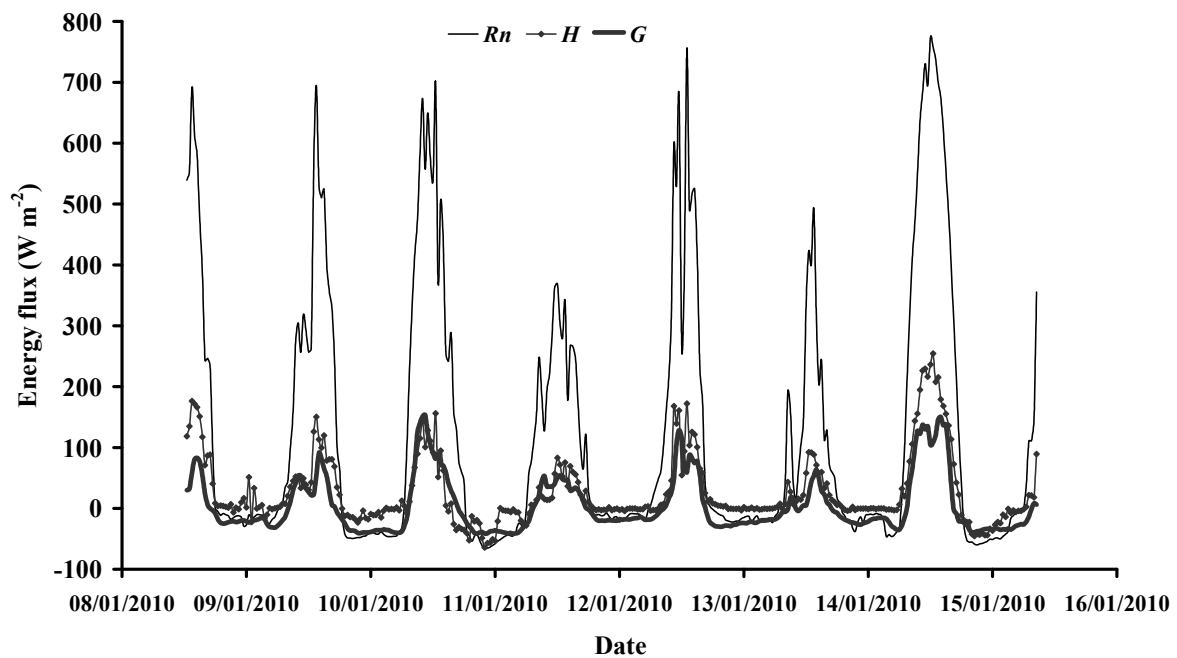


Figure 5.4. Diurnal variations of half-hourly net radiation (R_n), CSAT3 sonic anemometer sensible heat flux estimates (H_s) and the soil heat flux density (G) at the madumbe site for January 2010.

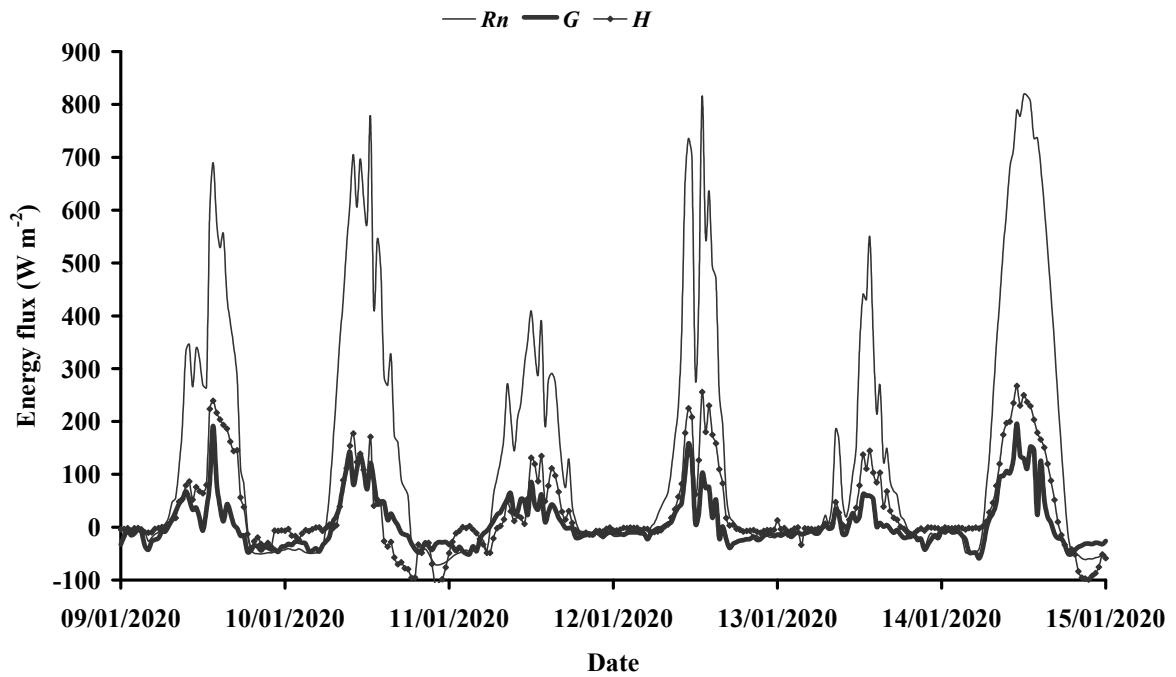


Figure 5.5. Diurnal variations of half-hourly net radiation (R_n), ATI sonic anemometer sensible heat flux estimates (H) and the soil heat flux density (G) at the sedge site for January 2010.

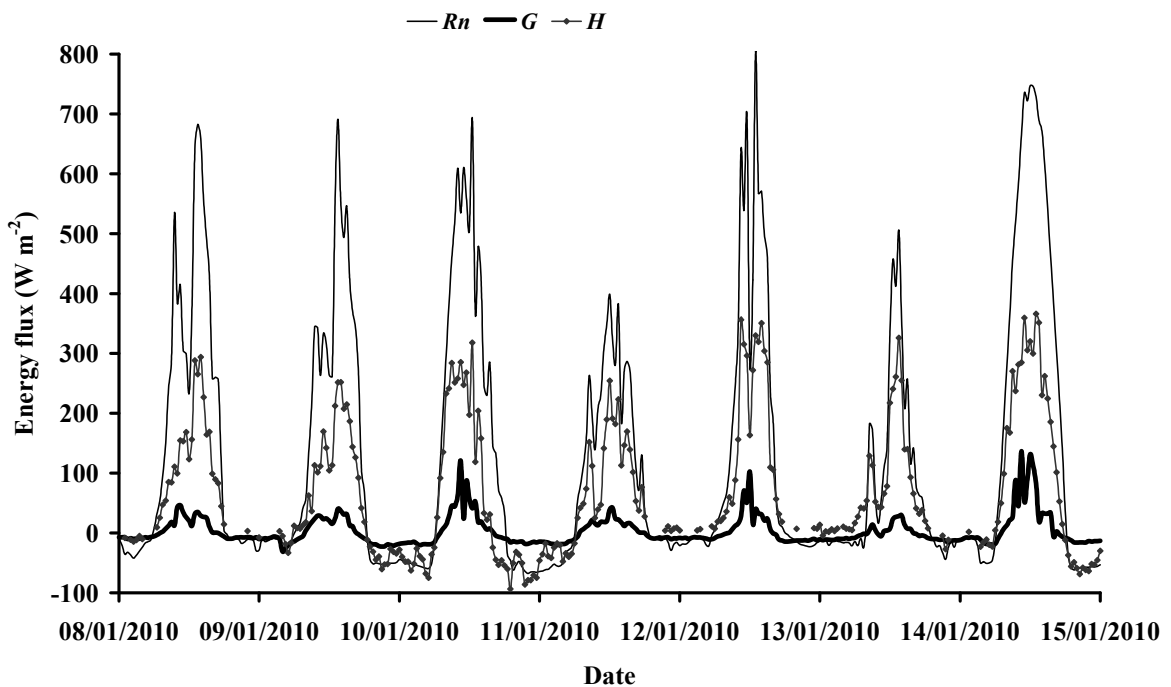


Figure 5.6. Diurnal variations of half-hourly net radiation (R_n), surface renewal (SR) sensible heat flux estimates (H), and the soil heat flux density (G) at the sugarcane site for January 2010.

5.3 Total Evaporation

5.3.1 First field campaign (20 to 26 November 2009)

The total daily evaporation at the madumbe site varied between a low of 2.3 mm day⁻¹ to a high of 4.8 mm day⁻¹. The average daily total evaporation for the four measurement days was 3.5 mm day⁻¹ (Figure 5.7). Total evaporation at the sedge site varied between 3.3 mm day⁻¹ to a high of 5.9 mm day⁻¹. The total daily evaporation at the sugarcane site varied between 2.6 mm and 4.8 mm. The average total evaporation estimates during these four days were 4.9 and 4.0 mm day⁻¹ for the sedge and sugarcane sites, respectively (Figure 5.7). The daily total evaporation at the madumbe site was lower than the sedge and sugarcane sites. This can be attributed to the low leaf area values of the madumbes. The madumbe plots were prepared by clearing the sedge and by creating furrows and raising planting beds to increase water flow from the fields. This altered the water balance of the plots by increasing the total evaporation during planting and making the soil drier for the growth stage of the madumbes during the November 2009 field campaign. Since the surface was dry, soil evaporation would not be expected to compensate for the low leaf area. Despite the availability of different methods for estimating ET, there is no single method or approach which is best for estimating ET accurately due to the variability and complexity of wetlands (Drexler *et al.*, 2004). In this study, two different eddy covariance systems and a surface renewal method were used which to some extent could be a source of variation on the ET estimates. However, studies by Drexler *et al.* (2004) and Jarman *et al.* (2009) showed that with the advancement of new technologies the variation in the ET estimates using these different methods is within 10 %.

The sugarcane canopy planted in the catchment around the wetland had a closed canopy with an average height of 1.65 m and the volumetric soil water content was greater than 35% at this site after two consecutive rainfall events prior to the measurement days. This could have resulted in higher daily total evaporation estimates from the sugarcane site compared to the madumbe site. Total evaporation estimates from the sedge were the highest (very close to ET_o) as a result of the high availability of water to the roots of the sedge which were submerged in water.

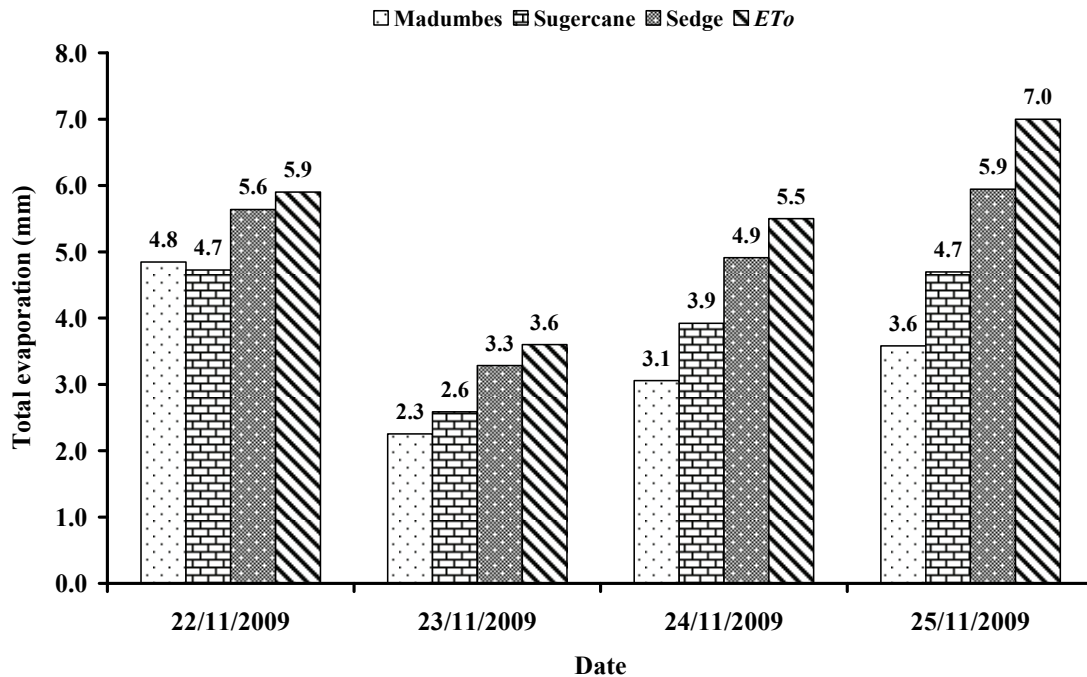


Figure 5.7. The daily total evaporation estimates at the madumbe, sedge, sugarcane sites and reference evapotranspiration (ET_o) (November 2009).

5.3.2 Second field campaign (8 to 15 January 2010)

The total daily evaporation at the madumbe site varied between 1.8 and 4.5 mm day⁻¹. The average daily total evaporation for the six measurement days was 3.3 mm day⁻¹ (Figure 9). Total evaporation at the sedge site varied between 1.8 mm day⁻¹ to a high of 5.4 mm day⁻¹. The total daily evaporation at the sugarcane site varied between 0.8 mm and 3.8 mm. The average total evaporation estimates were 3.7 and 2.4 mm day⁻¹ for the sedge and sugarcane sites, respectively (Figure 5.8). Total evaporation estimates from the sedge were the highest (close to ET_o) as a result of the high availability of water to the roots of the sedge which were submerged in water in the wetland. The daily total evaporation at the sugarcane site was lower than the sedge and madumbe sites, due to differences in soil water content between sites. For example, the sugarcane site volumetric water content was only 15% when compared to the 30% and 80% at the madumbe and sedge sites respectively.

The total evaporation estimates for the second field campaign (Figure 5.8) were lower than the first field campaign (November 2009) for madumbes, sedge and sugarcane. More variation in the available energy due to cloud cover (Figures 5.4, 5.5 and 5.6) and a decrease

in the volumetric soil water content at the three sites in January 2010 may have resulted in lower total evaporation rates.

5.4 Footprint of Measurements

As measurements were made in a field with limited fetch (60 m), a footprint analysis was undertaken to observe the relative contribution of upwind surface sources to the measured downwind sensible heat and latent energy fluxes. The footprint model developed by Hsieh *et al.* (2000), corrected and modified for a surface with a displacement height (d) and surface roughness length (z_o) (Savage *et al.*, 2004) was used to estimate relative contributions from areas at various upwind distances (x). The footprint calculations included footprint function (f) (Eq. 10), the cumulative fraction of the flux (F) to surface source flux (S_o) ratio (Eq. 12) and the peak location of the footprint (x_{peak}) (Eq. 13).

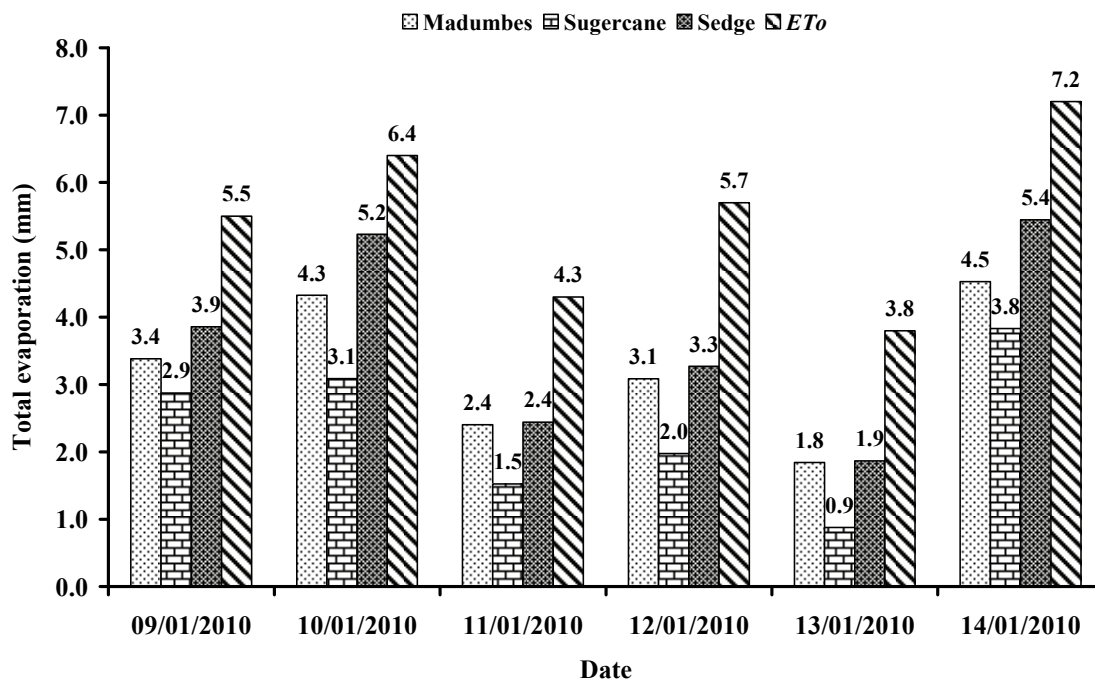


Figure 5.8. The daily total evaporation estimates at the madumbe, sedge, sugarcane sites and reference evapotranspiration (ET_o) (January 2010).

The footprint magnitude and the peak location of the footprint calculated using Obukhov length (L_o) values from the EC system at 1.10 m for unstable atmospheric conditions are shown in Figure 5.9 for 22 November ($L_o = -22.43$), 23 November ($L_o = -32.51$), 24 November ($L_o = -12.15$) and 25 November ($L_o = -14.23$) 2009. These footprint plots show that the peak location of the footprint (x_{peak}) varied from day to day depending on the atmospheric stability. The cumulative fraction of the measured flux (F) to surface source flux (S_o) ratio (Eq. 12) and the peak location of the footprint are presented in Figure 5.10 for the same four days in November 2009 for unstable conditions.

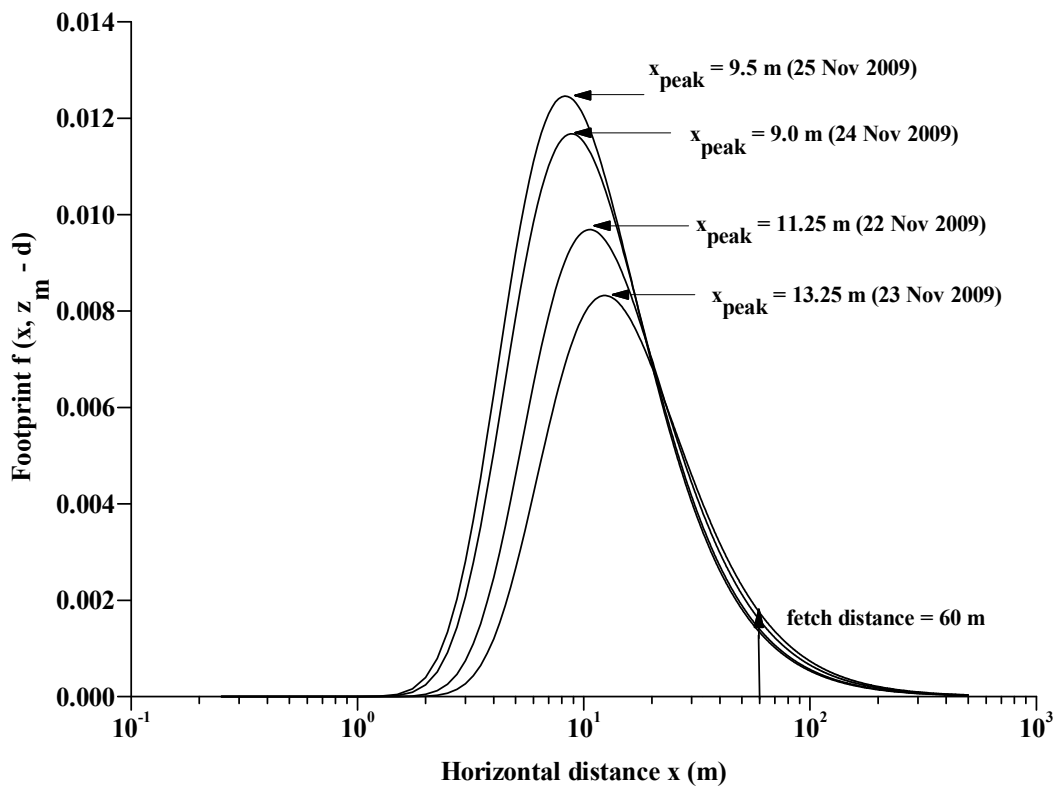


Figure 5.9. The estimated footprint and the peak location of the footprint at midday for four days in November 2009, based on the EC measurements at 1.10 m from the ground surface and horizontal distance x (m) from the measurement position.

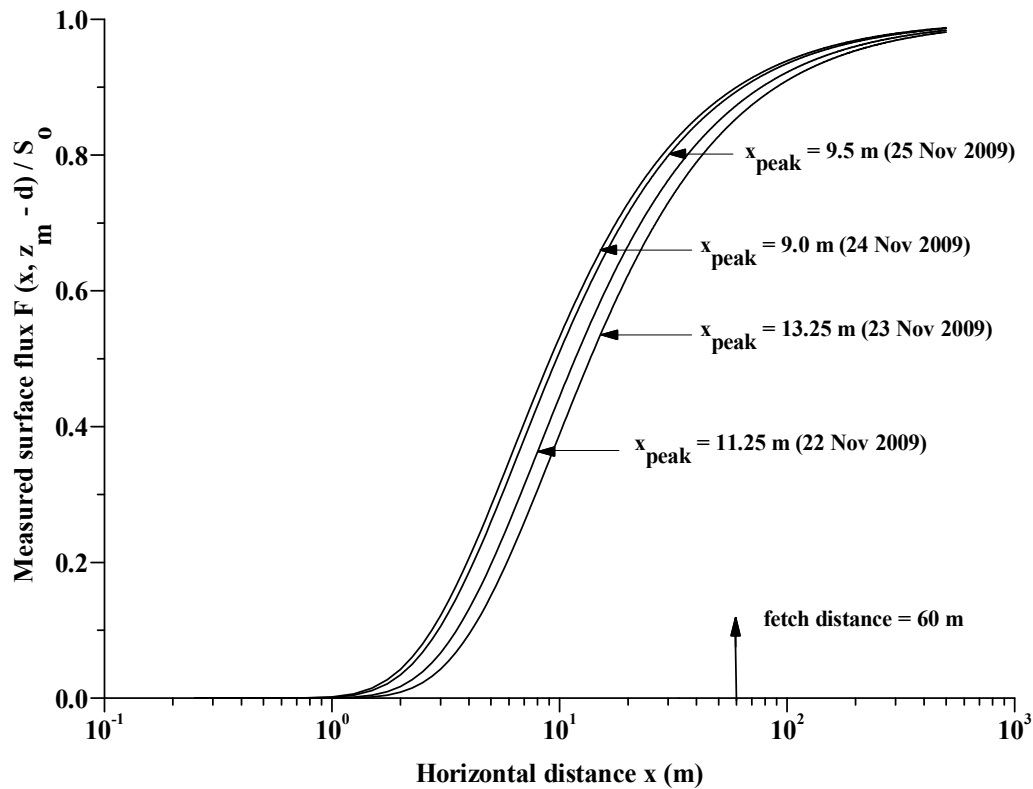


Figure 5.10. The cumulative fraction of the measured flux (F) to surface source flux (S_o) ratio and the peak location of the footprint at midday for four days in November 2009.

The footprint magnitude and the cumulative fraction of the measured flux (F) to surface source flux (S_o) ratio for the second field campaign – 09 January ($L_o = -64.84$), 10 January ($L_o = -33.09$), 11 January ($L_o = -38.22$) and 12 January ($L_o = -8.76$) 2010- are presented in Figures 5.11 and 5.12, respectively. The ratio of the measured flux (F) to surface source flux (S_o) is greater than 85% for most of the days and greater than 90% for 24 and 25 November 2009 and 12 January 2010 for a fetch distance (x) of 60 m for the site. Based on this analysis, more than 85% (close to 90%) of the measured flux was coming from the upwind fetch distance of 60 m. These footprint plots are calculated for unstable conditions during the peak hours of the measured fluxes. Therefore, the trend of the peak location of the footprint and the cumulative fraction of the measured flux (F) to surface source flux (S_o) ratio could be different for neutral and stable conditions. The footprint analysis presented in Figures 5.9, 5.10, 5.11 and 5.12 were made for unstable conditions using L_o values at 12h00. However,

atmospheric stability may vary occasionally during the day from unstable to near neutral to stable conditions. Under these generally windless conditions, fetch limitations would be less problematic and, therefore, we are 90% confident that the measurements made here are representative of the underlying canopy.

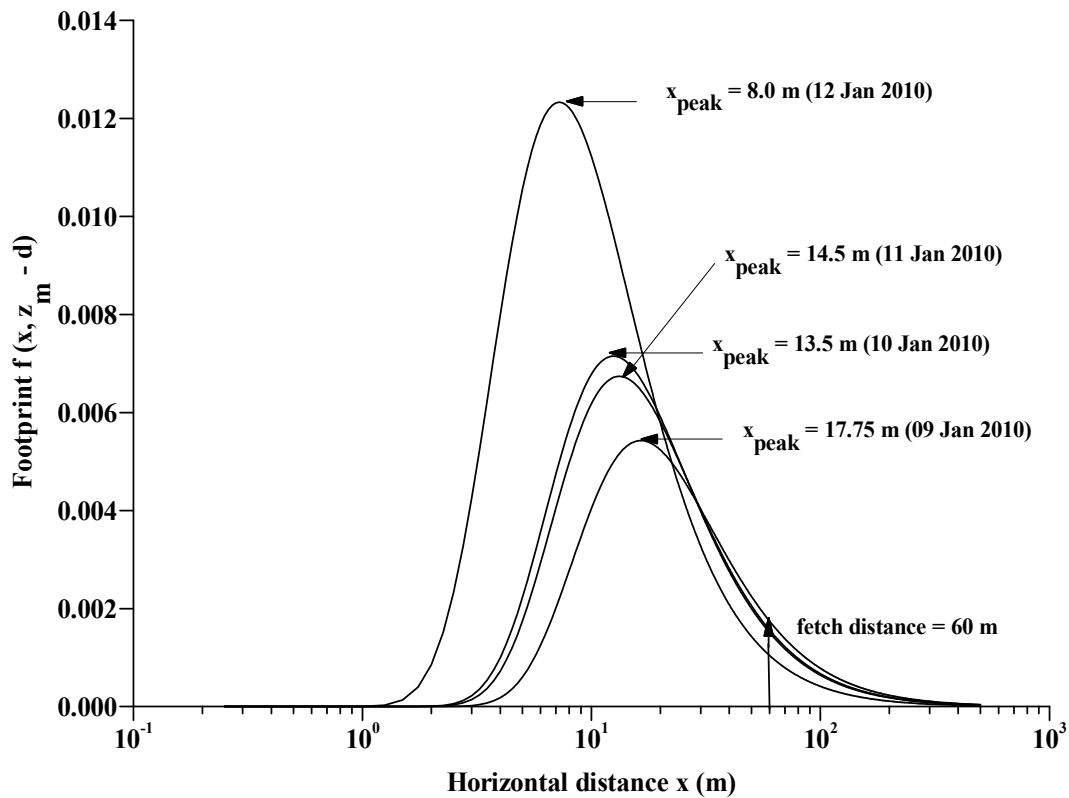


Figure 5.11. The estimated footprint and the peak location of the footprint at midday for four days in January 2010, based on the *EC* measurements at 1.30 m from the ground surface and horizontal distance x (m) from the measurement position.

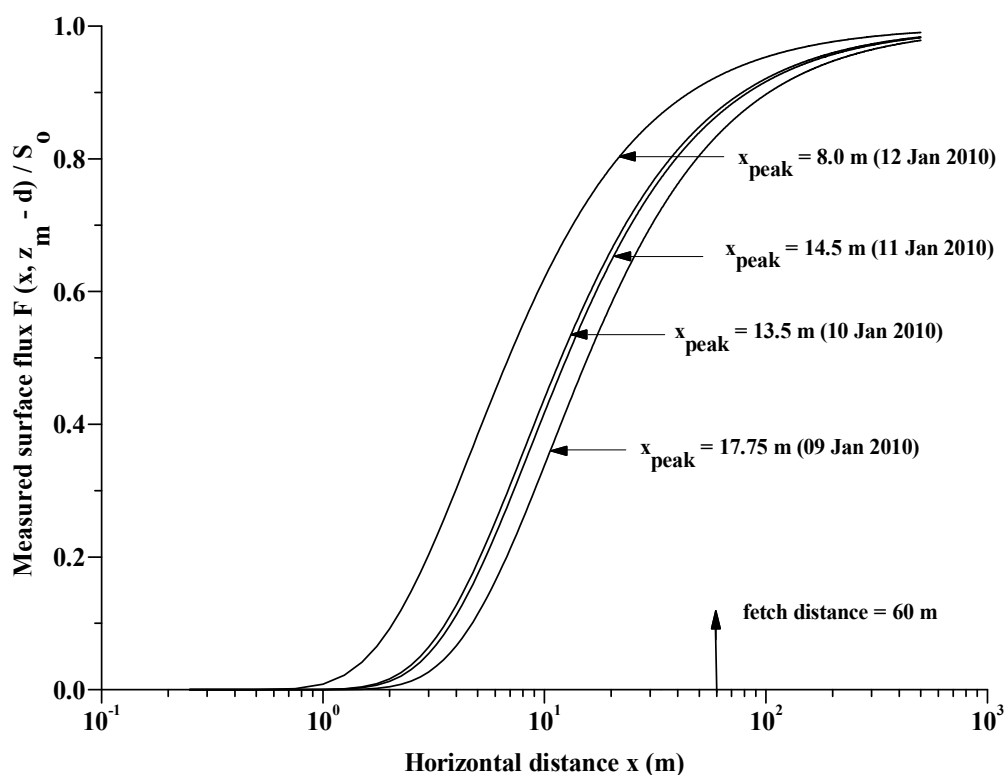


Figure 5.12. The cumulative fraction of the measured flux (F) to surface source flux (S_o) ratio and the peak location of the footprint at midday for four days in January 2010.

5.5 Water Use of Madumbes Using FAO-56 Penman-Monteith Model and Crop Factor

The actual ET was measured using the eddy covariance method for window periods during the growing season of the madumbes in November 2009 and January 2010. Continuous measurement of the actual ET was not possible due to financial reasons. Instead, meteorological data and the FAO-56 Penman-Monteith Equation were used to estimate reference evapotranspiration (ET_o) and, using a crop factor (K_c), the water use of madumbes was calculated for the growing season. The crop coefficient (K_c) of the madumbes was determined as the ratio of the measured ET using the eddy covariance system and ET_o from AWS data (Figure 14). The crop factor (K_c) depends on the type of crop, growth stage of the crop and climatic variables. An average madumbe crop factor value of 0.6 was obtained for both field campaigns in November 2009 and January 2010 (Figure 5.13). These data suggest

that the Madumbe plant is a conservative water user (i.e. it uses only 60% of ET_0) even though it grows in wet conditions. Day to day variation within November and January was generally less than 8%. The Madumbe growing season in KwaZulu-Natal is from November to March and we would therefore not expect the K_c values for the unmeasured months to differ much from those measured in November and January. Day to day variation within a season was generally $< 8\%$.

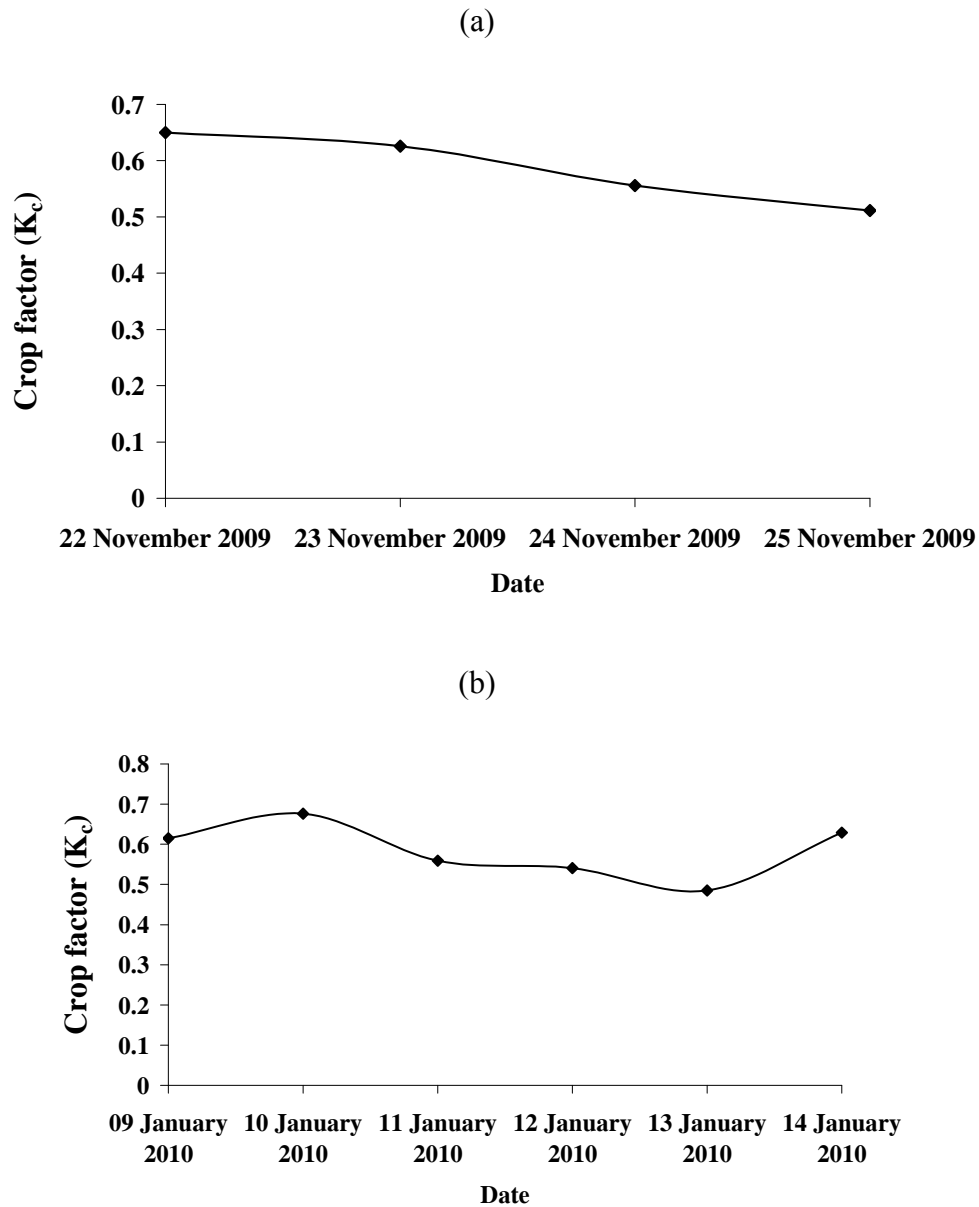


Figure 5.13. Crop factor (K_c) for the madumbes: (a) November 2009 and (b) January 2010.

Daily variations in ET_o , ET estimates from madumbes (using a crop factor $K_c = 0.6$) and rainfall are shown in Figure 5.14, for the three month period from November (2009) to January (2010). Evapotranspiration (ET) estimates varied from day to day depending on the available energy at the surface and soil water content. ET_o estimates varied from 1 to 10 mm and ET estimates from the madumbes ranged between 1 and 6 mm (Figure 5.14). Monthly total ET estimates from the madumbes were 72 mm (November 2009), 71 mm (December 2009), and 79 mm (January 2010). Monthly ET_o values varied from 120 mm, 118 mm and 132 mm for November and December 2009, and January 2010, respectively. The daily average ET estimates from madumbes (using ET_o with $K_c = 0.6$) were 2.5 mm (November 2009), 2.3 mm (December 2009) and 2.9 mm (January 2010).

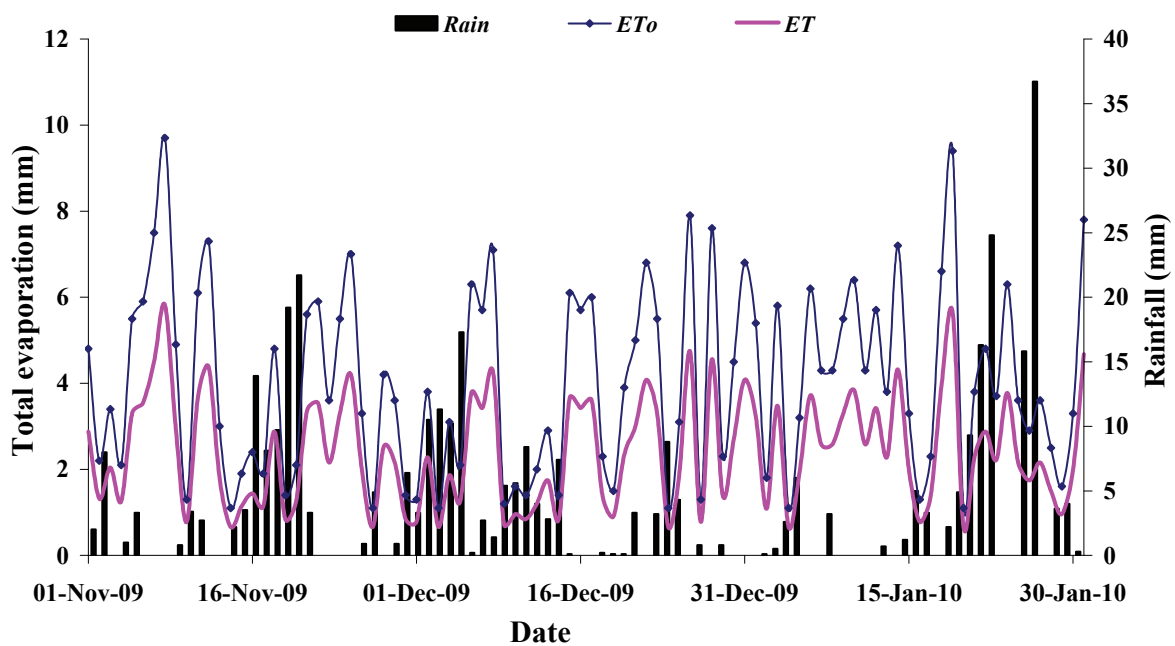


Figure 5.14. Daily variation in ET_o (mm), ET estimates from madumbes (using $K_c = 0.6$) and rainfall (mm) for November and December 2009, and January 2010.

6 CONCLUSION

This report describes two field campaigns made in November 2009 and January 2010 during the growing season of madumbes to quantify the total evaporation rates in the Mbongolwane wetland catchment over three vegetation types: madumbe (*Colocasia esculenta*), sedge (*Cyperus latifolius*) with some reeds (*Phragmites mauritianus*), and sugarcane.

The daily average total evaporation rates in November 2009 were 3.5, 4.0, and 4.9 mm for the madumbe, sugarcane, and sedge sites respectively. The daily average total evaporation rates in January 2010 were 3.3, 2.4 and 3.7 mm for the madumbes, sugarcane and sedge, respectively. The daily total evaporation was therefore lowest at the madumbe site in November 2009 and lowest at the sugarcane site later in the season in January 2010. The crop factor (K_c) is a coefficient that relates the measured ET to modelled ET_o . An average crop factor value of 0.6 was obtained from this study on the growth stage of the madumbes for both field campaigns in November 2009 and January 2010, which will be invaluable for future modelling the water use of madumbes and hydrologic water balance of the wetland.

The total evaporation rates in January 2010 were lower than in November 2009 for all three sites. A decrease in the available energy due to cloud cover and a decrease in the soil water content at the three sites resulted in the lower ET rates during the second field campaign. The soil heat flux plays an important role in the energy balance of wetlands as it is a large portion of the net radiation available at the wetland surface compared to dry-land where the soil heat flux is lower than 10% of the net radiation.

The madumbe plots were prepared by creating furrows and raising planting beds to increase water flow from the plots. This causes drying of the madumbe plots and affects the water balance of the wetland during planting and growing stages of the madumbe cultivation. We recommend long-term total evaporation measurements starting before the planting dates of the madumbes to thoroughly investigate the effects of the madumbe cultivation on the wetland. These field campaigns represent a unique set of high quality data and hopefully a basis for further studies on the impact of madumbe cultivation on wetlands.

7 REFERENCES

- Allen, RG, Pereira, LS, Raes, D and Smith, M. (1998). Crop evapotranspiration: guidelines for computing crop water requirements. FAO Irrigation and Drainage Paper No. 56, Rome, Italy.
- Arya, SP. (2001). *Introduction to Micrometeorology*. Second edition. Academic Press. London, UK.
- Birkhead, AL, James, CS, Kleynhans, MT. (2007). Hydrological and hydraulic modelling of the Nyl River floodplain Part 2: Modelling hydraulic behaviour. *Water SA* 33(1):9-20.
- Bullock, A. (1992). Dambo hydrology in southern Africa – review and reassessment. *Journal of Hydrology* 134:373-396.
- Bullock, A and Acreman, M. (2003). The role of wetlands in the hydrological cycle. *Hydrology and Earth Systems Sciences* 7(3):358-389.
- Dingman, SL. (2002). *Physical Hydrology*. Second edition. New Jersey: Prentice Hall.
- Drexler, JZ, Snyder, RL, Spano, D, Paw, KT. (2004). A review of models and micrometeorological methods used to estimate wetland evapotranspiration. *Hydr. Proc.* 18:2071-2101.
- Drexler, JZ, Anderson, FE, Snyder, RL. (2008). Evapotranspiration rates and crop coefficients for a restored marsh in the Sacramento-San Joaquin Delta, California, USA. *Hydr. Proc.* 22:725-735.
- Fermor, P, Hedges, D, Gilbert, JC, and Gowing, DJG. (2001). Reedbed evapotranspiration rates in England. *Hydro. Proc.* 15:621-631.
- Finnigan, JJ. (2004). The footprint concept in complex terrain. *Agric. For. Meteorol.* 127: 117-129.

- Gao, W, Shaw, RH and Paw U, KT. (1989). Observation of organized structure in turbulent flow within and above a forest canopy. *Boundary-Layer Meteorol.* 47:349-377.
- Gash, JHC (1986). A note on estimating the effect of a limited fetch on micrometeorological evaporation measurements. *Boundary-Layer Meteorol.* 35:409-413.
- Grenfell, MC, Ellery, WN and Preston-Whyte, RA. (2005). Wetlands as early warning (eco)systems for water resource management. *Water SA* 31(4):465-471.
- Horst, TW and Weil JC. (1992). Footprint estimation for scalar flux measurements in the atmospheric surface-layer. *Boundary-Layer Meteorol.* 59:279-296.
- Hsieh C, Katul, G, Chi, T. (2000). An approximate analytical model for footprint estimation of scalar fluxes in thermally stratified atmospheric flows. *Adv. Water Resour.* 23:765-772.
- Jacobs, JM, Mergelsberg, SL, Lopera, AF and Myers, DA. (2002). Evapotranspiration from a wet prairie wetland under drought conditions: Paynes Prairie Reserve, Florida, USA. *WETLANDS* 22(2):374-385.
- Jarmain, C, Everson, CS, Savage, MJ, Mengistu, MG, Clulow, AD, Walker, S, Gush, MB. (2009). Refining tools for evaporation monitoring in support of water resources management. Report No. 1567/1/08: 137 pp, ISBN 978-1-77005-798-2. Water Research Commission, Pretoria, South Africa.
- Kaimal, JC and Finnigan, JJ. (1994). *Atmospheric Boundary Layer Flows, Their Structure and Measurement*. Oxford University Press, New York, USA.
- Koerselman, W, Beltman, B. (1988). Evapotranspiration from fens in relation to Penman's potential free water evaporation ($E_{sub(o)}$) and pan evaporation. *Aqu. Bot.* 31(3-4):307-320.
- Kotze, DC, Memela B, Fuzani N and Thobela, M. (2002). Utilization of the Mbongolwane wetland in KwaZulu-Natal, South Africa. International Water Management Institute, Pretoria.

- Leclerc, MY and Thurtell, GW. (1990). Footprint prediction of scalar fluxes using a Markovian analysis. *Boundary-Layer Meteorol.* 52:247-258.
- McCartney, MP. (2000). The water budget of a headwater catchment containing a dambo. *Phys. Chem. Earth (B)* 25(7-8):611-616.
- Meyers, TP and Baldocchi, DD. (2005). Current micrometeorological flux methodologies with applications in agriculture. In: Hatfield, JL, Baker, JM (Eds.).date? *Micrometeorology in Agricultural Systems. Agronomy Monograph* 47:381-396.
- Pasquill, F. (1972). Some aspects of boundary layer description. *Quart. J Roy. Meteorol. Soc.* 98:469-494.
- Paw U, KT, Brunnet, Y, Collineau, S, Shaw, RH, Maitani, T, Qui, J and Hippias, L. (1992). On coherent structure in turbulence within and above agricultural plant canopies. *Agric. For. Meteorol.* 61:55-68.
- Paw U, KT, Qui, J, Su, HB, Watanabe, T and Brunnet, Y. (1995). Surface renewal analysis: a new method to obtain scalar fluxes. *Agric. For. Meteorol.* 74:119-137.
- Paw U, KT, Snyder, RL, Spano, D and Su, HB. (2005). Surface renewal estimates of scalar exchange. In: Hatfield, JL and Baker, JM (Eds). *Micrometeorology in Agricultural Systems. Agro. Mono.* 47:455-483.
- Raupach, MR, Finnigan, JJ and Brunet, Y. (1989). Coherent eddies in vegetation canopies. In: eds + name, *Proc. 4th Australasian Conf. on Heat and Mass Transfer*, pp75-90 . Bergell House, New York. USA.
- Rosenberg N J, Blad B L, Verma S B, 1983. *Microclimate: The Biological Environment*, 2nd ed., John Wiley and Sons Inc., New York, 495pp.

- Savage, MJ, Everson, CS and, Metelerkamp, BR. (1997). *Evaporation measurement above vegetated surfaces using micrometeorological techniques*. Report No. 349/1/97: 248 pp, ISBN 1-86845 363 4. Water Research Commission, Pretoria, South Africa.
- Savage, MJ, Everson, CS, Odhiambo, GO, Mengistu MG and Jarman, C. (2004). *Theory and practice of evapotranspiration measurement, with special focus on SLS as an operational tool for the estimation of spatially-averaged evaporation*. Report No.1335/1/04:204 pp, ISBN No: 1-77005-247-X. Water Research Commission, Pretoria, South Africa.
- Schmid, HP. (2002). Footprint modelling for vegetation atmosphere exchange studies: a review and perspective. *Agric. For. Meteorol.* 113:159-183.
- Snyder, RL, Spano, D and Paw U,KT. (1996). Surface renewal analysis for sensible heat and latent heat flux density. *Boundary-Layer Meteorol.* 77:249-266.
- Spano D, Snyder, RL, Duce P and Paw U, KT. (1997). Surface renewal analysis for sensible heat flux density using structure functions. *Agric. For. Meteorol.* 86:259-271.
- Spano D, Snyder, RL, Duce P and Paw U, KT. (2000). Estimating sensible and latent heat flux densities from grape vine canopies using surface renewal. *Agric. For. Meteorol.* 104:171-183.
- Sun, L and Song, C. (2008). Evapotranspiration from a freshwater marsh in the Sanjiang Plain, Northeast China. *Journal of Hydrology* 352:202-210.
- Swinbank, WC. (1951). Measurement of vertical transfer of heat and water vapour by eddies in the lower atmosphere. *J. Meteorol.* 8:135-145.
- Van Atta, CW. (1977). Effect of coherent structures on structure functions of temperature in the atmospheric boundary layer. *Arch. Mech.* 29:161-171.

Ward, AD and Trimble, SW. (2004). *Environmental Hydrology*. Lewis Publishers, CRC Press, Boca Raton, Florida, USA.